Author Manuscript

Title: Hierarchical Spin-Crossover Cooperativity in Hybrid 1-D Chains of FeII-1,2,4-trizole Trimers Linked by [Au(CN)2]- Bridges

Authors: Lida Ezzedinloo; Katrina A. Zenere; Zixi Xie; Manan Ahmed; SynØve Scottwell; Mohan Bhadbhade; Helen E. A. Brand; Jack K. Clegg; Carol Hua; Natasha F. Sciortino; Lachlan C. Parker; Benjamin J. Powell; Cameron J. Kepert; Suzanne M Neville

To be cited as: 10.1002/chem.202100358

Link to VoR: https://doi.org/10.1002/chem.202100358

COMMUNICATION

Hierarchical Spin-Crossover Cooperativity in Hybrid 1-D Chains of Fe^{II}-1,2,4-trizole Trimers Linked by $[Au(CN)_2]^-$ Bridges

Lida Ezzedinloo, Katrina A. Zenere, Zixi Xie, Manan Ahmed, Synøve Scottwell, Mohan Bhadbhade, Helen E. A. Brand, Jack K. Clegg, Carol Hua, Natasha F. Sciortino, Lachlan C. Parker, Benjamin J. Powell, Cameron J. Kepert and Suzanne M. Neville*

Abstract: *Foremost, practical applications of spin-crossover (SCO) materials require control of the nature of the spin-state coupling. In existing SCO materials, there is a single, well-defined dimensionality relevant to the switching behavior. We show that a new material, consisting of 1,2,4-trizole-based trimers coordinated into 1-D chains by $[Au(CN)_2]^-$ and spaced by anions and exchangeable guests, undergoes SCO defined by elastic coupling across multiple dimensional hierarchies. Detailed structural, vibrational, and theoretical studies conclusively confirm that intra-trimer coupling is an order of magnitude greater than the intra-molecular coupling, which is an order of magnitude greater than inter-molecular coupling. As such, we have ascertained for the first time a clear hierarchy on the nature of elastic coupling in SCO materials, a necessary step for the technological development of molecular switching materials.*

It has long been considered that the molecular bistability observed in spin-crossover (SCO) materials makes them viable for applications such as optical and memory devices.[1] However, the fact that SCO is elastic in origin,[2] and hence closely tied to the lattice and its hierarchy of interactions, means that device suitable preparations, such as Langmuir-Blodgett films and nanoparticles dispersion,[3] are challenging, in particular with respect to retention of key application criteria (ambient switching and wide hysteresis loops).[1] To this end, $[Fe^{II}(R\text{-}trz)_3](A)_2{\cdot}xH_2O$ (Figure 1a, R = 4-substituent, A = monovalent anion) chains have been widely explored as they intrinsically support abrupt transitions with thermal hysteresis.[1a,4] These features are thought to arise from strong interchain and weaker intermolecular interactions.[5] The spin transition characteristics within this family can be varied from extremely abrupt (occurring over a few K), to moderately abrupt (occurring over 10-30 K), to smooth (occurring over 30 – 100 K) by R-substituent and anion variation and the degree of hydration.[4f] Key points with respect to device implementation are that the chains are charged, and interchain interactions (direct and electrostatic) are necessary for producing hysteretic character,[2a-b,5] and that chain length shortening has been shown to weaken solid-state cooperativity.[4e] Collectively, these constitute a substantial technological hurdle if the fabrication of electronic devices is to be achieved.[1]

Hence, with a vision towards downsizing for application, it is necessary to uncover model systems with which to probe the relative effect of intra- and inter-molecular elastic coupling and substantiate the importance of local interchain interaction pathways. This is particularly important for $[Fe^{II}(R\text{-}trz)_3](A)_2{\cdot}xH_2O$ systems, as they do not tend to form as single crystals, so detailed structural information are not directly accessible.[4g-h] The trimer complex $[Fe_3(bntrz)_6(tcnset)_6]$ (1,2,4-triazole and cyanidocarbanion ligands),[6] has provided some information on intra-trimer cooperativity, as, in contrast to other trinuclear 1,2,4-triazole families[7] where it is only the central Fe^{II} site in each trimer which undergoes SCO, all three Fe^{II} sites show a cooperative spin-state transition. Detailed structural analyses[6] indicate that these trimers act as correlated entities but with more moderate inter-trimer cooperativity, which is consistent with the hydrogen-bonding inter-trimer connectivity. However, the neutrality of $[Fe_3(bntrz)_6(tcnset)_6]$[6] and the lack of lattice solvent does not allow comprehensive comparison to $[Fe^{II}(R\text{-}trz)_3](A)_2{\cdot}xH_2O$ species.[4] To this end, here, we present a new optimal model system for quantifying and disentangling the relative intra- and inter-molecular elastic contributions of relevance to the $[Fe^{II}(R\text{-}trz)_3](A)_2{\cdot}xH_2O$ family.[4] This new material is comprised of Fe^{II}-1,2,4-triazole trimers (Figure 1a) directly bridged by $[Au(CN)_2]^-$ units; this results in anionic 1-D chains (Figure 1c) spaced by anions and exchangeable guest species. As such, this new material can be considered as hybrid between $[Fe^{II}(R\text{-}trz)_3](A)_2{\cdot}xH_2O$[4] and Hofmann-type frameworks[8] with $[Au(CN)_2]^-$ bridges (Figure 1), both of which have been the subject of extensive studies as they show ambient switching and high cooperativity. Through a range of structural, magnetic, spectroscopic, and elastic modelling we distinguish the relative nature and magnitude of intra- and inter-molecular coupling, all of which directly clarifies the observed SCO behaviours across the $[Fe^{II}(R\text{-}trz)_3](A)_2{\cdot}xH_2O$ family. Of novelty, the elastic couplings operate at different energetic and dimensional length-scales, namely, strong intra-trimer (0-D), moderate inter-trimer (1-D) and weaker inter-chain (3-D) couplings, providing key information on the nature and hierarchy of elastic interactions. These findings have broad implications for allowing fine control of the nature of spin-state coupling necessary for the technological development of molecular switching materials.[1]

[*] L. Ezzedinloo, M. Ahmed, S. Scottwell, S. M. Neville, The School of Chemistry, The University of New South Wales, Sydney 2052, Australia. Email: s.neville@unsw.edu.au.
K. A. Zenere, Z. Xie, N. F. Sciortino, C. J. Kepert, The School of Chemistry, The University of Sydney, Sydney 2006, Australia.
M. Bhadbhade Mark Wainwright Analytical Centre, The University of New South Wales, Sydney 2052, Australia
H. E. Brand, Australian Synchrotron, ANSTO Clayton, Victoria 3800, Australia.
J. K. Clegg, School of Chemistry and Molecular Biosciences, The University of Queensland, St Lucia 4072, Australia
C. Hua, School of Chemistry, The University of Melbourne, Parkville 3010, Australia
L. C. Parker, B. J. Powell, School of Mathematics and Physics, The University of Queensland, St Lucia 4072, Australia.
Supporting information and the ORCID idenfication numbers for the authors of this

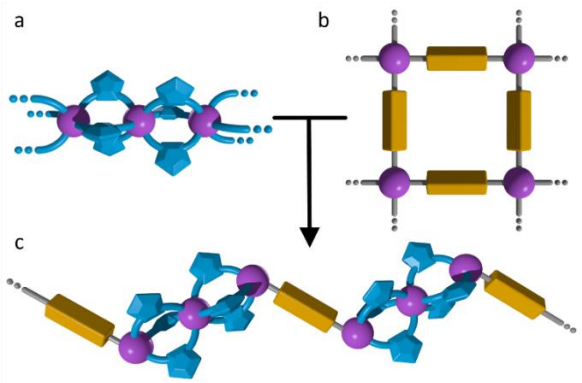

Figure 1. Schematic of (a) 1-D chains of the composition [Fe^{II}(R-1,2,4-triazole)$_3$]anion, (b) Hofmann layer of the type [$Fe^{II}(Au(CN)_2)_2$] and (c) 'Hybrid' 1-D chains of the type [Fe^{II}_3(R-1,2,4-triazole)$_8(Au(CN)_2)_4$]·$(Au(CN)_2)_2$·guest.

Crystals of [$Fe_3(bztrz)_8(Au(CN)_2)_4$]·2{$Au(CN)_2$}·guest, **A**·guest (guest = $4H_2O$ and $2(H_2O{\cdot}MeOH)$), were readily produced over a period of 4 weeks by slow evaporation of a mixture of $Fe(ClO_4)_2{\cdot}6H_2O$, $K[Au(CN)_2]$ and bztrz ((E)-1-phenyl-N-(1,2,4-triazol-4-yl)-methanimine).[9] With a 1:1 MeOH:H_2O or ~7:1 MeOH:H_2O solution **A**·$4H_2O$ and **A**·$2(H_2O{\cdot}MeOH)$ are produced, respectively. With heating (400 K), the solvent-free phase **A**·Ø is produced in a single-crystal to single-crystal transformation. **A**·guest is comprised of trimers of Fe^{II} sites bridged by bztrz $\mu_{1,2}$-1,2,4-triazole groups (Figure 2a); the central Fe^{II} site (Fe2) is coordinated by six triazole groups, reminiscent of 1-D chain[4] and trinuclear[7] 1,2,4-triazole families. The outer Fe^{II} sites (Fe1) are coordinated by three $\mu_{1,2}$-1,2,4-triazole groups, one unidentate triazole nitrogen atom from a bztrz ligand and two $[Au(CN)_2]^-$ anions. Half of the coordinated $[Au(CN)_2]^-$ anions act as bridges between trimers to form 1-D chains (Figure 2c). These cationic chains are packed in parallel (Figure 2c) and interact via a range of supramolecular contacts (Figure 2b; Tables S3-4), such as Au···Au interactions between the unbound and bridging $[Au(CN)_2]^-$ anions and CN···C(H) interactions with triazole groups from adjacent trinuclear units. Distinguishing **A**·$4H_2O$ and **A**·$2(H_2O{\cdot}MeOH)$ are the guests; for both the water molecules interact with the terminal $[Au(CN)_2]^-$ anions (Figure 2a, CN···OH_2). The remaining guest molecules reside in small pockets between adjacent 1-D chains (Figure S13-14) and interact with the free $[Au(CN)_2]^-$ anions. The trinuclear units in both **A**·$4H_2O$ and **A**·$2(H_2O{\cdot}MeOH)$ lie on an inversion centre, giving two crystallographically distinct Fe^{II} sites per trinuclear unit (i.e., [Fe1–Fe2–Fe1']; Figure 2a). Guest removal to produce **A**·Ø occurs in parallel with a crystallographic phase transition (confirmed *via* single crystal (Table S2) & powder diffraction, Figure 3b:inset), yielding a trinuclear unit which sits on a general position and consequently contains three distinct Fe^{II} sites (i.e., [Fe1–Fe2–Fe3]). The overall trimer and 1-D chain structure is virtually unchanged with guest removal, aside from the rotation of one of the benzene groups around the imine bond (Figure S11). Hirshfeld surface analyses[10] (Figure S28-30) also confirm minor variation to the packing and contacts.

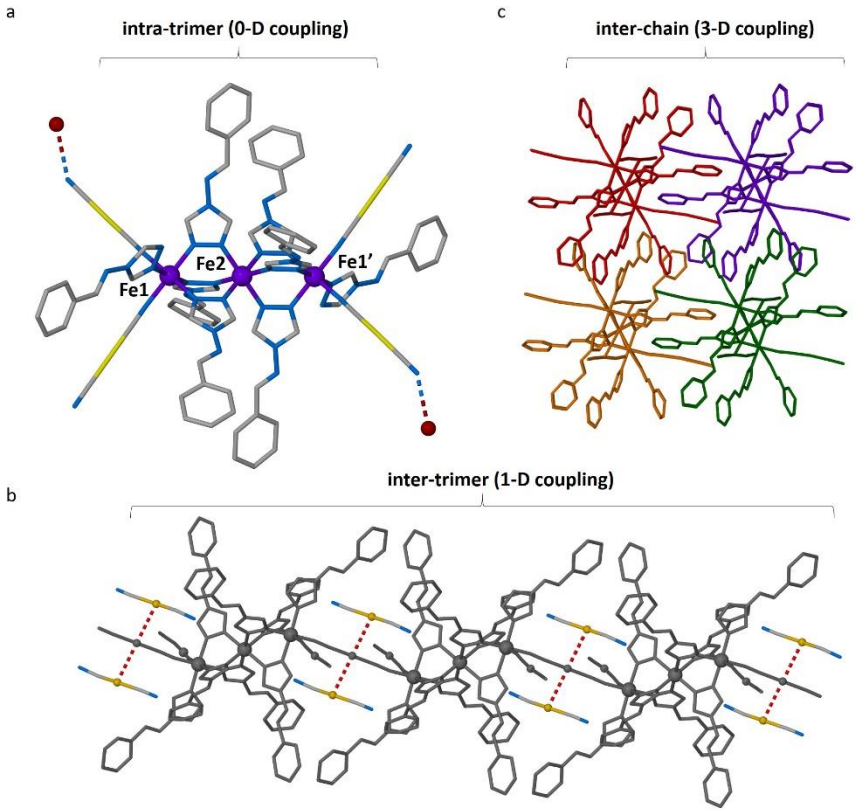

Figure 2. (a) The $[Fe_3(bztrz)_8(Au(CN)_2)_4]^{2+}$ trinuclear unit, water molecules (red sphere) and interactions indicated; the Fe^{II} sites within each trimer show strong elastic coupling such that they act as a 0-D correlated entity. (b) The 1-D chain structure $[Fe_3(bztrz)_8(Au(CN)_2)_4]{\cdot}2\{Au(CN)_2\}$·guest (**A**·guest; guest = $2(H_2O{\cdot}MeOH)$, $4H_2O$) and Au…Au (red); the strongly correlated trimers (0-D) are connected into chains (1-D) by $[Au(CN)_2]^-$ coordination bridges thereby defining a strong 0-D → moderate 1-D structural and elastic heirarchy. (c) The anionic 1-D chains (parallel packed along the *c*-axis) are dispersed by uncoordinated $[Au(CN)_2]^-$ anions and guest molecules; these form weaker 3-D communication pathways. Hence this structure is defined by an overall strong 0-D → moderate 1-D → weak 3-D structural and elastic coupling heirarchy.

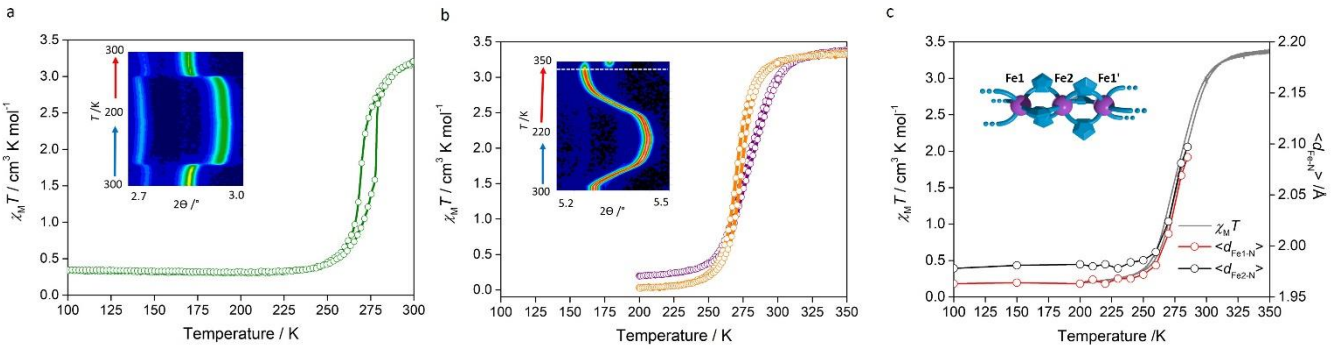

Figure 3. $\chi_M T$ versus temperature plot for (a) **A**·4H$_2$O (green; 300–100–300 K; 1 Kmin^{-1}) and (b) **A**·2(H$_2$O·MeOH) (purple) & **A**·Ø (orange) (350–200–350 K; 1 Kmin^{-1}). Inset: Powder X-ray diffraction peak position evolution. (c) Average Fe-N bond lengths variation (<d_{Fe-N}>) versus temperature for **A**·2(H$_2$O·MeOH); the $\chi_M T$ versus temperature plot included for comparative purposes. Inset: Structural schematic showing placement of Fe1 and Fe2 in each trimer. Note: the temperature scale is different for **A**·4H$_2$O to clarify the hysteresis loop.

Variable temperature magnetic susceptibility data for **A**·4H$_2$O, **A**·2(H$_2$O·MeOH) and **A**·Ø reveal one-step SCO transitions (Figure 3a-b), but with variation in transition temperature, curve abruptness and thermal hysteresis; corresponding variable temperature powder diffraction measurements (Figures 3a-b:inset) reproduce these trends and demonstrate that the behaviours are intrinsic to the bulk materials rather than arising from any degree of sample heterogeneity. For each material, the onset of the LS to HS transition occurs at approximately the same temperature (*ca*. 250 K). The LS ↔ HS transition of **A**·4H$_2$O occurs over the smallest temperature range (*ca*. 250 – 300 K), and hence displays the most abrupt transition of the series ($T_{½}\downarrow\uparrow$ = 270, 278 K; Figure 3a). A thermal hysteresis in the heating and cooling curves (ΔT = 8 K) is observed for **A**·4H$_2$O. The LS ↔ HS transition of **A**·2(H$_2$O·MeOH) occurs over the broadest temperature range in the series (*ca*. 250 – 325 K), with negligible thermal hysteresis ($T_{½}\downarrow\uparrow$ = 276, 278 K; Figure 3b, S26). Guest removal results in a sharpening of the transition curve (*ca*. 250 – 310 K; **A**·Ø: $T_{½}\downarrow\uparrow$ = 272, 275 K). Therefore, in the context of [Fe^{II}(R-trz)$_3$](A)$_2$·*x*H$_2$O,[4] the transition behaviour of **A**·4H$_2$O can be considered as moderately cooperative, and **A**·2(H$_2$O·MeOH) and **A**·Ø more weakly cooperative, in terms of the temperature range their transitions.[4f] Given the majority of [Fe^{II}(R-trz)$_3$](A)$_2$·*x*H$_2$O materials[4] display the former, ascribed to strong intrachain and weaker interchain interactions, detailed investigation of the nature and magnitude of these structural features is important to probe here.

To quantify the cooperativity across the **A**·guest series, the SCO curves were analysed using the 1-D Ising-Wajnflasz-Pick model.[11] This pure 1-D approach provided a much better fit than a mean-field theory (i.e., the Slichter-Drickamer model, Figure S35),[12] which is more appropriate in higher dimensions, and provides additional information on intra- and intermolecular contributions compared to the phenomenological domain model.[13] For **A**·guest, the experimental $\chi_M T$ values were fit (Figure S31-33) assuming that all three Fe^{II} sites within each trimer have the same spin-states, as indicated by their one-step transition characters. The results show that the enthalpy and entropy difference between HS and LS states trimers across the **A**·guest series are $\Delta H \simeq 29$ kJmol^{-1} and $\Delta S \simeq 100$ JK^{-1}mol^{-1}, respectively. These values are in agreement with DSC data performed on **A**·4H$_2$O and **A**·2(H$_2$O·MeOH) ($\Delta H \simeq 34$ kJmol^{-1}, $\Delta S \simeq 113$ JK^{-1}mol^{-1}, per trimer) and are comparable to those of [Fe$_3$(bntrz)$_6$(tcnset)$_6$] (54 kJ mol^{-1} and 170 J mol^{-1} K^{-1}, per trimer)[6] and [Fe^{II}(R-trz)$_3$](A)$_2$·*x*H$_2$O examples which show moderate to weak cooperativity (10 – 30 kJmol^{-1} and 50 – 100 Jmol^{-1}K^{-1}, per Fe^{II} site).[4c] This is consistent with the presence of a bulky R-group in **A**·guest, which is thought to prevent densification of inter-chain interactions in the [Fe^{II}(R-trz)$_3$](A)$_2$·*x*H$_2$O family, leading to reduced hysteresis effects.[4c]

Of considerable importance, the 1-D Ising-Wajnflasz-Pick model[11] has provided information on the relative energy-scales of intra-trimer ($J_0 \gg \Delta H$, as we do not find significant numbers of mixed spin-state trimers, see below), inter-trimer (i.e., chain, $J_\parallel$) and inter-chain ($J_\perp$) interaction strengths across the **A**·guest series. We find that $J_\parallel$ varies by almost a factor of two ($J_\parallel = 1.9$ kJ mol^{-1} in **A**·4H$_2$O, $J_\parallel = 1.55$ kJ mol^{-1} in **A**·Ø, and $J_\parallel = 1.0$ kJ mol^{-1} in **A**·2(H$_2$O·MeOH)) across the **A**·guest series, showing that the changes in crystal packing due to the guests significantly impact the degree of cooperativity in the SCO transition. Nevertheless, the energy scale of intra-trimer coupling (ΔH) is an order of magnitude greater than that of inter-trimer coupling ($J_\parallel$). Furthermore, including inter-chain coupling ($J_\perp$) at the mean-field level induces the hysteresis seen experimentally, and we find that its energy-scale is again diminished compared to that of the intra-trimer and inter-trimer interactions (Table S5). This is clear evidence that the intra-chain connectivity dominates the sharp spin-state transition and that the transition character (such as smooth versus abrupt, with or without thermal hysteresis) is defined by subtleties of inter-chain interactions, in particular inter-chain coupling;[14] all of which has thus far only been theorised in [Fe^{II}(R-trz)$_3$](A)$_2$·*x*H$_2$O materials.[2a-b,5]

The (mean-field) Slichter-Drickamer model has previously been used to demonstrate a correlation in the [Fe^{II}(R-trz)$_3$](A)$_2$·*x*H$_2$O family between ΔH and the cooperativity parameter $\Gamma = 4J_\parallel$ for our quasi-1D model.[4c] **A**·2(H$_2$O·MeOH) fits well with the trend found for the [Fe^{II}(R-trz)$_3$](A)$_2$·*x*H$_2$O family. As varying the guest can increase Γ by almost a factor of two without changes ΔH (or ΔS), this demonstrates that the unique dimensional hierarchy of the **A**·guest system allows us to fine tune the degree of

cooperativity in the SCO transition independent of other changes.

To corroborate the hierarchy of interactions obtained by modelling, we interrogate the relative structural variation over the spin-state transition with respect to intra-trimer, inter-trimer and interchain interaction pathways. The intra-trimer cooperativity was probed by variable temperature single crystal data collected on **A**·2(H_2O·MeOH) at fine temperature intervals (100–285 K; Table S1). A plot of the temperature-dependence of the Fe–N bond lengths attained from single crystal data shows a parallel spin-state transition at both the Fe1 and Fe2 sites (Figure 3c). While these variable temperature structural studies indicate that the trimer Fe^{II} sites switch cooperatively, these data (as per single crystal data on $[Fe_3(bntrz)_6(tcnset)_6]$[6] are also consistent with a thermal mixture of, for example, [HS-LS-HS], [LS-HS-LS], [LS-LS-HS], [LS-HS-HS] at the intermediate region, and so do not preclude the existence of a range of local mixed spin-state trimers which would disprove the strong intra-trimer coupling. To explore this further, variable temperature vibrational spectroscopy, which unlike diffraction measurement is sensitive to the local trimer spin-state rather than the spatial average attained by diffraction measurements, was employed on **A**·2(H_2O·MeOH). The spectra (Figure S27) indicate that a clean conversion occurs between the [LS-LS-LS] and [HS-HS-HS] trimer states, with an absence of any features that could be attributable to mixed spin-state trimers. We can therefore conclude with certainty that the transition of the inequivalent Fe^{II} sites within each local trimer occurs simultaneously, rather than *via* a mixture of thermally-populated or elastically-coupled mixed trimer states. Therefore, theory and experiment confirm that that the trimers act as strongly correlated units which define the concerted one-step spin-state transition, and implies that strong intrachain coupling is achieved in all the $[Fe^{II}(R\text{-}trz)_3](A)_2{\cdot}xH_2O$ series irrespective of oligomer length, R-substituent, anion and degree of hydration.[4]

The more moderate nature of the intra-trimer coupling evidenced by the 1-D Ising-Wajnflasz-Pick model[9] of **A**·guest, is evidenced experimentally by the increase in both the intra- and inter-trimer Fe-Fe distances over the LS to HS transition (Tables S3-4). This is opposed to $[Fe_3(bntrz)_6(tcnset)_6]$,[6] where the trimer communication is via hydrogen-bonding and the intra-trimer Fe-Fe distance increase, but the inter-trimer distances decrease over the LS to HS transition. This indicates that inter-trimer hydrogen bonds act to 'cushion' the LS to HS transition rather than aiding in transmission.[2] The nature of the inter-trimer contribution in **A**·guest is further supported by the pronounced growth of the *c*-axis (i.e., the 1-D chain length) over the LS to HS transition, compared to that of the *a*- and *b*-axes (Figure S3; $\Delta c/c$ is four times greater than $\Delta a/a$ and two times greater than $\Delta b/b$). This is in line with structural studies on $[Fe^{II}(R\text{-}trz)_3](A)_2{\cdot}xH_2O$ systems.[4g-h] The finding that the coupling here via $[Au(CN)_2]^-$ coordination bridges is more moderate than via short, rigid triazole bridges, gives some indication that the strong cooperativity observed in Hofmann frameworks arises from a bulk effect rather than from local structural features.[8,14]

Beyond establishing the nature and relative magnitude of intra-trimer (0-D) and inter-trimer (1-D) coupling, the cationic nature of the chains, the presence of anions and solvent in the lattice and the stability of **A**·guest to solvent variation (**A**·2(H_2O·MeOH), **A**·4H_2O and **A**·Ø) provides a novel added platform to substantiate the relative role of different interchain (inter-molecular) interactions on SCO character. Notably, as the $[Fe^{II}(R\text{-}trz)_3](A)_2{\cdot}xH_2O$ family are poorly crystalline, this information is not directly attainable, other than via comparison of SCO characters of anion and guest varied species. Structural information attained from a low-resolution crystal structure of one member of the $[Fe^{II}(R\text{-}trz)_3](A)_2{\cdot}xH_2O$ family,[4g-h] indicates a dense network of interchain interactions involving the triazole ligands, the anions, and the water molecules. Given that the interchain interactions are necessary to reproduce the abrupt and hysteretic transitions,[2a-b,5] it is important to establish their specific molecular-scale role.[14] Qualitatively, the variation to SCO behaviour in the $[Fe^{II}(R\text{-}trz)_3](A)_2{\cdot}xH_2O$ series[4] derives from electrostatic contributions[5] and the ability of the chains to interact most efficiently, hence why ligand steric bulk has a negative effect as do larger anions.[4f] Indeed, in **A**·4H_2O, which shows the greatest thermal hysteresis of the **A**·guest family, structural analysis shows that the chains in are more efficiently packed; this is likely driven by the achievement of shorter host-guest interactions and reduced guest bulk than for example **A**·2(H_2O·MeOH). Despite the absence of guests in **A**·Ø, the packing is slightly less efficient than **A**·4H_2O, indicating that the water interactions are necessary for inducing thermal hysteresis. These findings and the factor of two changes in $J_{\|}$ support the thus far hypothesized impact of R-substituent, anion and guest variation in $[Fe^{II}(R\text{-}trz)_3](A)_2{\cdot}xH_2O$[4] on interchain interaction capacity and therefore the long-range cooperativity, to enhance or temper hysteretic effects.

To conclude, this new family of materials has provided a rare insight into the nature and relative magnitude of different modes of elastic coupling in SCO 1-D chains. This important study has been afforded by the unique modular discrete cluster + coordination polymer network structural platform derived from Fe^{II} trinuclear species, bridged by linear $[Au(CN)_2]^-$ units into 1-D chains and spaced by anions and exchangeable guest species. Notably, this construct contains structural features of direct relevance for the highly studied $[Fe^{II}(R\text{-}trz)_3](A)_2{\cdot}xH_2O$ family, namely Fe^{II} sites bridged by triazole ligands, the cationic nature of the chains and the presence of anions and guests in the lattice. It also contains $[Au(CN)_2]^-$ bridges which are said to be responsible for the highly cooperative SCO transitions in Hofmann-type frameworks. Through a series of detailed theoretical and experimental studies, we can definitively conclude that the short, rigid triazole bridges act to afford strong coupling, such that the trimers undergo spin-state transition as a cohesive unit. Beyond this, we have shown that the strongly correlated trimers are more moderately coupled along the length of the 1-D chains, as facilitated by the $[Au(CN)_2]^-$ coordination

bridges, and more weakly coupled by interchain interactions via the anion and guest species. All this information directly feeds into the hypothesised strength and role of intra- and inter-molecular elastic interaction contributions of the $Fe^{II}(R\text{-}trz)_3](A)_2{\cdot}xH_2O$ family, which have not been clearly evidenced due to the weakly crystalline nature of this family. Of note, we find that both intra-molecular and inter-molecular interactions are contributors to the SCO properties, but act at different magnitudes, therefore, conclusively disentangling the relative nature and contributions of these structural features at the molecular-scale. This study has also allowed a hierarchy of elastic coupling over multiple dimensions to be defined for the first time, i.e., strong intra-trimer (0-D) → moderate inter-trimer (1-D) → weak inter-chain (3-D). In most materials, there is a single, well-defined dimensionality due to the nature of elastic coupling at the molecular level, there is a unique hierarchy of dimensional scales due to the multiple structural connectivity's which act with distinct elastic coupling energies. Collectively, these findings have implications for allowing fine control of the nature of spin-state coupling at the molecular-level, a necessary step if the technological development of molecular switching materials is to progress beyond current nanostructuring strategies. With a broader vision, this study opens the way to a vast family of 1-D chain SCO materials, which are highly crystalline and chemically tuneable (R-substituent, anion, guests) for which to further probe elastic interactions. Of particular interest will be the study of these chain species with less bulky 4-substituents towards achieving wide hysteresis at room temperature.

Acknowledgements

We acknowledge support from Fellowships and Discovery Project funding from the Australian Research Council (ARC). Access and use of the facilities of the Australian Synchrotron was supported by ANSTO. JKC acknowledges the support of the ARC through LE170100144. We thank Ross McKenzie for helpful conversations.

Keywords: spin crossover • triazole • cooperativity • hierarchy • 1-D chain

1. (a) O. Kahn, Molecular Magnetism, VCH, New York, **1993**; (b) P. Gütlich, P., A. Hauser, H. Spiering, H., *Angew. Chem., Int. Ed.*, **1994**, *33*, 2024; (c) O. Kahn, C. J. Martinez, *Science*, **1998**, *279*, 44–48; (d) P. Gütlich, Y. Garcia, T. Woike, *Coord. Chem. Rev.*, **2001**, *219–221*, 839; (e) J.-F. Létard, P. Guionneau, L. Goux-Capes, *Top. Curr. Chem.*, **2004**, *235*, 221–249; (f) M. A. Halcrow, Spin-crossover materials: properties and applications, John Wiley & Sons, Ltd, **2013**; (h) X. Bao, H. J. Shepherd, L. Salmon, G. Molnár, M.-L. Tong, A. Bousseksou, *Angew. Chem. Int. Ed.* **2013**, *52*, 1198-1202; (i) P. Gütlich, A. B. Gaspar, Y. Garcia, Y., *Beilstein J. Org. Chem.*, **2013**, *9*, 342–391; (j) O. Sato, *Nat. Chem.*, **2016**, *8*, 644–656; (k) C.-M. Jureschi, J. Linares, A. Boulmaali, P. R. Dahoo, A. Rotaru, Y. Garcia, *Sensors*, **2016**, *16(2)*, 187; (l) K. Senthil Kumar, M. Ruben, *Coord. Chem. Rev.* **2017**, *346*, 176–205; (m) V. Rubio-Giménez, C. Bartual-Murgui, M. Galbiati, A. Nuñez-López, J. Castells-Gil, B. Quinard, P. Seneor, E. Otero, P. Ohresser, E. Coronado, J. A. Real, R. Mattana, S. Tatay, C. Marti-Gastaldo, *Chem. Sci.*, **2019**, *10*, 4038-47.

2. (a) J. Linares, H. Spiering, F. Varret, *Eur. Phys. J. B* **1999**, 10, 271-275; (b) K. Boukheddaden, J. Linares, H. Spiering, F. Varret, *Eur. Phys. J. B* **2000**, *15*, 317–326; (c) H. Spiering, *Top. Curr. Chem.*, **2004**, 171–195; (d) M. Nishino, K. Boukheddaden, Y. Konishi, S. Miyashita, *Phys. Rev. Lett.*, **2007**, *98*, 247203; (e) K. Boukheddaden, S. Miyashita, M. Nishino, *Phys. Rev. B*, **2007**, *75*, 094112; (f) M. Nishino, K. Boukheddaden, S. Miyashita, *Phys. Rev. B*, **2009**, *79*, 012409; (g) M. Paez-Espejo, M. Sy, K. Boukheddaden, *J. Am. Chem. Soc.*, **2016**, *138*, 3202–3210; (h) J. Cruddas, B. J. Powell, *J. Am. Chem. Soc.*, **2019**, *141*, 19790–19799; (g) J. Cruddas, B. J. Powell, *Inorg. Chem. Front.*, **2020**, *7*, 4424–4437.

3. (a) O. Roubeau, A. Colin, V. Schmitt, R. Clerac, *Angew. Chem., Int. Ed.* **2004**, *43*, 3283–3286; (b) T. Fujigaya, D.-L. Jiang, T. Aida, *Chem. Asian J.* **2007**, 2, 106–113; (c) O. Roubeau, E. Natividad, B. Agricole, S. Ravaine, *Langmuir*, **2007**, *23*, 3110–3117; (d) O. Roubeau, B. Agricole, R. Clerac, S. J. Ravaine, *Phys. Chem. B*, **2004**, *108*, 15110–15116; (e) E. Coronado, J. R. Galan-Mascaros, M. Monrabal-Capilla, J. García-Martínez, R. Pardo-Ibanez, *Adv. Mater.* **2007**, *19*, 1359–1361; (f) T. Forestier, S. Mornet, N. Daro, T. Nishihara, S.-I. Mouri, K. Tanaka, O. Fouche, E. Freysz, J.-F. Letard, *Chem. Commun.* **2008**, 432–4329.

4. (a) J. Kröber, J. P. Audiére, R. Claude, E. Codjovi, O. Kahn, J. G. Haasnoot, F. Groliére, C. Jay, A. Bousseksou, J. Linarés, F. Varret, A. Gonthier-Vassal, *Chem. Mater.*, **1994**, *6*, 1404–1412; (b) Y. Garcia, P. J. van Koningsbruggen, R. Lapouyade, L. Fournès, L. Rabardel, O. Kahn, V. Ksenofontov, G. Levchenko, P. Gütlich, *Chem. Mater.*, **1998**, *10*, 2426–2433; (c) O. Roubeau, M. Castro, R. Burriel, J. G. Haasnoot, J. Reedijk, *J. Phys. Chem. B*, **2011**, *115*, 3003; (d) G. J. Haasnoot, *Coord. Chem. Rev.* **2000**, *200-202*, 131–185; (e) O. Roubeau, J. M. Alcazar Gomez, E. Balskus, J. J. Kolnaar, J. G. Haasnoot, J. Reedijk, *New J. Chem.*, **2001**, *25*, 144–150; (f) O. Roubeau, *Chem. Eur. J.* **2012**, *18*, 15230–15244; (g) A. Grosjean, N. Daro, B. Kauffman, A. Kaiba, J.-F. Létard, P. Guionneau, *Chem. Commun.* **2011**, *47*, 12382–12384; (h) A. Grosjean, P. Négrier, P. Bordet, C. Etrillard, D. Mondieig, S. Pechev, E. Lebraud, J.-F. Létard, P. Guionneau, *Eur. J. Inorg. Chem.* **2013**, *2013*, 796–802; (i) M. M. Dîrtu, A. D. Naik, A. Rotaru, L. Spinu, D. Poelman, Y. Garcia, *Inorg. Chem.* **2016**, *55*(9), 4278-4295; (j) M. B. Bushuev, D. P. Pishchur, I. V. Korolkov, K. A. Vinogradova, *Phys. Chem. Chem. Phys.* **2017**, *19*, 4056–4068.

5. M. Kepenekian, B. Le Guennic, V. Robert, *J. Am. Chem. Soc.*, **2009**, *131*(32), 11498-11502.

6. N. Pittala, F. Thétiot, C. Charles, S. Triki, K. Boukheddaden, G. Chastanet, M. Marchivie, *Chem. Commun*. **2017**, *53*, 8356-8359.

7. (a) G. Vos, R. A. Le Febre, R. A. G. de Graff, J. G. Haasnoot, J. Reedijk, *J. Am. Chem. Soc.*, **1983**, 105, 1682; (b) ; G. Vos, R. A. G. de Graaff, J. G. Haasnoot, A. M. van der Kraan, P. de Vaal, J. Reedijk, *Inorg. Chem.*, **1984**, 23, 2905-10; (c) M. Thomann, O. Kahn, J. Guilhem, F. Varret, *Inorg. Chem.*, **1994**, 33, 6029-37; (d) J. J. A. Kolnaar, G. van Dijk, H. Koojiman, A. L. Spek, V. Ksenofontov, P. Gütlich, J. G. Haasnoon, J. Reedijk, *Inorg. Chem.*, **1997**, 36, 2433; (e) Y. Garcia, P. Guionneau, G. Bravic, D. Chasseau, J. A. K. Howard, O. Kahn, V. Ksenofontov, S. Reiman, P. Gütlich, *Eur. J. Inorg. Chem.* **2000**, *2000*, 1531–1538; (f) D. Savard, C. Cook, G. D. Enright, I. Korobkov, T. J. Burchell, M. Murugesu, *CrystEngComm.*, **2011**, 13, 5190-97; (g) V. Gómez, J. Benet-Buchholz, E. Martin, J. R. Galán-Mascarós, *Chem. Eur. J.* **2014**, *20*(18), 5369–5379; (h) W.-B. Chen, J.-D. Leng, Z.-Z. Wang, Y.-C. Chen, Y. Miao, M.-L. Tong, W. Dong, *Chem. Commun.* **2017**, *53*, 7820-7823; (i) Y. M. Klein, N. F. Sciortino, C. E. Housecroft, C. J. Kepert, S. M. Neville, *Magnetochem.*, **2016**, 2, 7; (j) W.-B. Chen, Y.-C. Chen, M. Yang, M.-L. Tong, W. Dong, *Dalton Trans.*, **2018**, *47*, 4307-4314; (k) A. Moneo-Corcuera, D. Nieto-Castro, C. S. de Piaón, V. Gómez, P. Maldonado-Illescas, J. R. Galan-Mascaros, *Dalton Trans.*, **2018**, 47, 11895-11902; (l) I. Sánchez-Molina, A. Moneo-Corcuera, D. Nieto-Castro, J. Benet-Buchholz, J. R. Galán-Mascarós, *Eur. J. Inorg. Chem.*, **2020**, 2, 112-116.

8. (a) J. A. Real, A. B. Gaspar, V. Niel, M. C. Muñoz, *Coord. Chem. Rev.*, **2003**, *236*, 121–141; (b) J. A. Real, A. B. Gaspar, M. C. Muñoz, *Dalton Trans.*, **2005**, 2062; (c) V. Niel, J. M. Martinez-Agudo, M. C. Muñoz, A. B. Gaspar, J. A. Real, *Inorg. Chem.* **2001**, *40*, 3838–3839; (c) M. C. Muñoz, J. A. Real, *Coord. Chem. Rev.*, **2011**, *255*, 2068-2093; (d) Z.-P. Ni, J.-L. Liu, N. Hoque, W. Liu, J.-Y. Li, Y.-C. Chen, M.-L. Tong, *Coord. Chem. Rev.* **2017**, *335*, 28-43.

9. M. J. Murphy, K. A. Zenere, F. Ragon, P. D. Southon, C. J. Kepert, S. M. Neville, *J. Am. Chem. Soc.*, **2017**, 139, 1330–1335.

10. M. A. Spackman, J. J. McKinnon, *CrystEngComm*, **2002**, *4*, 378-392.

11. (a) J. Wajnflasz, R. Pick, *J. Phys. Colloques* **1971**, *32*, C1-91–C1–92; (b) J. Pavlik, R. Boča, *Eur. J. Inorg. Chem*., **2013**, *2013*, 697-709; (c) K. Boukheddaden, S. Miyashita, M. Nishino, *Phys. Rev. B*, **2007**, *75*, 094112; (d) J. Linares, H. Spiering, F. Varret, *Eur. Phys. J. B* **1999**, *10*, 271-275.

12. C. P. Slichter, H. G. Drickamer, *J. Chem. Phys.* **1972**, *56*, 2142– 2160.

13. (a) M. Sorai, S. J. Seki, *J. Phys. Chem. Solids*, **1974**, *35*, 555–570; (b) M. Sorai, *Top. Curr. Chem.* **2004**, *235*, 153–170.
14. M. G. Reeves, E. Tailleur, P. A. Wood, M. Marchivie, G. Chastanet, P. Guionneau, S. Parsons, *Chem. Sci.*, **2020**, 12, 1007-1015.

.

Table of Contents

Hierarchical cooperativity. Crucial information on the nature, magnitude, and dimensional hierarchy of elastic coupling in spin-crossover systems has been achieved in a family of materials consists of trimers linked into coordination chains and spaced by anions and exchangeable guests.